NASA Technical Paper 2079

September 1982

A New Measurement Method for Separating Airborne and Structureborne Noise Radiated by Aircraft-Type Panels

Michael C. McGary

NASA

NASA
Technical
Paper
2079

1982

A New Measurement Method for Separating Airborne and Structureborne Noise Radiated by Aircraft-Type Panels

Michael C. McGary
Langley Research Center
Hampton, Virginia

National Aeronautics
and Space Administration

**Scientific and Technical
Information Branch**

SUMMARY

This paper presents the theoretical basis and experimental validation of a new measurement method for separating airborne and structureborne noise radiated by aircraft-type panels. The method is an extension of the two-microphone, cross-spectral acoustic intensity measurement method combined with existing theory-of-sound radiation of thin-shell structures of various designs. The method is restricted to the frequency range below the coincidence frequency of the structure. Consequently, the method lends itself to low-frequency noise problems such as propeller harmonics.

Measurements were performed on both an aluminum sheet and on two built-up aircraft-panel designs (i.e., two aluminum panels with frames and stringers) with and without added damping. The results of the measurements indicate that this new method is a viable option to the other diagnostic tools currently available.

INTRODUCTION

The interior noise levels of propeller-driven aircraft are substantially higher than the noise levels measured for other types of conventional take-off and landing (CTOL) aircraft. (See refs. 1 and 2.) The interior noise spectra of these aircraft are characterized by low-frequency discrete tones. The most bothersome of these discrete tones (harmonics of the engine firing frequency and propeller blade-passage frequency) typically range in frequency from 80 to 1000 Hz and in levels of sound pressure from 84 to 104 dB.

Reduction of the interior noise of propeller-driven aircraft requires a knowledge of the relative importance of the acoustic and structural noise transmission paths. Noise entering the aircraft interior via an acoustic path shall subsequently be referred to as the airborne noise. Noise entering the aircraft interior via a structural path shall subsequently be referred to as the structureborne noise. Current published research on the relative importance of airborne and structureborne noise in propeller-driven aircraft has sometimes culminated with differing conclusions. (See refs. 2 to 7.) Some of this apparent disagreement arises from shortcomings in the methods used for identifying the dominant noise paths. Two noise source and/or path identification methods that have been applied recently are the lead-wrapping method (ref. 8) and the partial and/or multiple coherence function methods (refs. 9 to 11). Attempts to identify noise paths in aircraft by lead-wrapping methods have proved unsatisfactory because of the poor transmission loss of lead at low frequency. The use of partial and/or multiple coherence functions to determine the principal noise paths in aircraft proves inadequate if the various noise-generating mechanisms of the aircraft are coherent.

Recently, several new noise source and/or path identification tools have come into widespread use. Among the most promising of these new tools are several methods for measuring the acoustic intensity vector. (See refs. 12 to 26.) In the past 2 years, researchers have begun to apply these methods to noise-transmission problems in aircraft. (See refs. 27 to 30.) The purpose of this paper is to present a new measurement method for separating airborne and structureborne noise radiated by

aircraft-type panels by using a two-microphone, cross-spectral acoustic intensity measuring device. The theoretical basis of the measurement method and the results of several tests designed for its validation are presented.

SYMBOLS

C_{pv}	real part of cross spectrum between pressure and velocity
c	speed of sound in acoustic medium
E	total vibrational energy of structure
f	frequency
$\vec{I}$	acoustic intensity vector
P	Fourier transform of acoustic pressure
p	instantaneous acoustic pressure
Q_{12}	imaginary part of cross spectrum between microphones 1 and 2
Re	real part
Δr	spacing between microphones for acoustic intensity probe
S	surface area
V	Fourier transform of acoustic particle velocity
v	normal surface velocity of structure
$\vec{v}$	instantaneous acoustic-particle-velocity vector
Π	sound power radiated by surface area
ρ	density of acoustic fluid medium
σ	acoustic radiation efficiency
ω	angular frequency
$\langle\ \rangle$	averaged quantity (over space or time)
$\lvert\ \rvert$	magnitude of a vector or complex number
$*$	complex conjugate

Subscripts:

a airborne component

s structureborne component

t time

THEORY OF MEASUREMENT METHOD

The measurement method is based on the theory of sound radiation of thin-shell structures of various designs. The acoustic radiation efficiency σ of some localized surface area of a thin-shell structure is defined as

$$\sigma = \frac{\Pi}{\rho c \langle v^2 \rangle S} \tag{1}$$

where $\langle v^2 \rangle$ is the space-averaged, mean-square normal surface velocity of area S and ρc is the characteristic acoustic impedance of the acoustic fluid medium. The radiation efficiency σ can be thought of as the ratio of the acoustic power radiated by a vibrating structure to the amount of acoustic power that would be produced by an acoustic plane-wave generator of the same area having the same space-averaged, mean-square surface velocity as the vibrating structure. By expressing the sound power Π in equation (1) as the product of the acoustic intensity vector (measured at the surface) with the surface area of the structure, the equation for radiation efficiency can be rewritten as

$$\sigma = \frac{|\vec{I}|}{\rho c \langle v^2 \rangle} \tag{2}$$

The acoustic intensity vector $\vec{I}$ is defined by the equation

$$\vec{I} = \langle p\vec{v} \rangle_t \tag{3}$$

In the frequency domain, the equation for intensity is given by

$$|\vec{I}(f)| = \mathrm{Re}[P(f)\ V^*(f)] = C_{pv}(f) \tag{4}$$

where $P(f)$ is the complex Fourier transform of the pressure and $V^*(f)$ is the complex conjugate of the Fourier transform of the acoustic particle velocity.

The equations for acoustic radiation efficiencies of thin-shell structures can be found in the literature. (For example, see refs. 31 and 32.) Discussions in

reference 31 point out that below the coincidence frequency of a thin-shell structure, the radiation efficiencies for an acoustic input and a vibrational input are different. This difference in radiation efficiencies is associated with the difference in compressional wavespeed in air and flexural wavespeed in the structure. Below coincidence frequency, a vibrational input produces flexural waves in the structure that travel at subsonic speeds. These slower flexural waves (sometimes referred to as free waves) are poor radiators of sound. An acoustic input, however, produces flexural waves in the structure that travel at speeds greater than or equal to the speed of sound. These fast flexural waves (sometimes referred to as forced waves) radiate sound very efficiently.

A rigorous explanation of the difference in airborne and structureborne radiation efficiencies for thin-shell structures can be made in terms of the vibrational modes of the structure. The response of a thin-shell structure to any type of input (acoustic or vibrational) can always be mathematically expressed as the superposition of a series expansion of the flexural mode shapes of the structure. Each mode shape in the series expansion will be multiplied by an "influence" coefficient that is uniquely associated with that particular mode. These influence coefficients determine the relative amount of "control" or "influence" that each individual mode retains over the total response of the structure. If the response is controlled by vibrational modes whose resonance frequencies are within the frequency band of excitation, the response is said to be "resonance controlled." If the response is controlled by vibrational modes whose resonance frequencies are below the frequency band of excitation, the response is said to be "mass controlled."

The response of a thin-shell structure to a point vibrational input is primarily resonance controlled in frequency bands well above the fundamental resonant frequency. Below coincidence frequency, a resonance-controlled panel response is a very inefficient noise generator (acoustically slow). The response of a thin-shell structure to an acoustic input can be either resonance controlled or mass controlled. Below the coincidence frequency, the response of a panel to an acoustic input is primarily mass controlled and is a very efficient noise generator (acoustically fast). Recently, Forssen and Crocker (ref. 33) have experimentally demonstrated this difference in the airborne and structureborne radiation efficiencies on panels at frequencies below coincidence by using a two-microphone, cross-spectral acoustic intensity measuring device.

The total sound power radiated by a structure can be written as

$$\Pi = \Pi_a + \Pi_s \tag{5}$$

By dividing by the surface area of the structure, equation (5) becomes

$$|\vec{I}| = |\vec{I}_a| + |\vec{I}_s| \tag{6}$$

By utilizing equation (2), equation (6) can then be written in terms of the acoustic intensity averaged over space and time as

$$|\vec{I}| = \sigma_a \rho c \left\langle v_a^2 \right\rangle + \sigma_s \rho c \left\langle v_s^2 \right\rangle \tag{7}$$

or

$$\frac{|\vec{I}|}{\rho c} = \sigma_a \langle v_a^2 \rangle + \sigma_s \langle v_s^2 \rangle \tag{8}$$

Similarly, the total vibrational energy in the structure can be written as

$$E = E_a + E_s \tag{9}$$

If the mass terms which are common to all three terms in equation (9) are cancelled, an equation can be written in terms of the space-averaged, mean-square surface velocities of the structure as

$$\langle v^2 \rangle = \langle v_a^2 \rangle + \langle v_s^2 \rangle \tag{10}$$

If equations (8) and (10) are solved simultaneously for the airborne and structure-borne mean-square surface velocities, the results are, respectively,

$$\langle v_a^2 \rangle = \frac{\sigma_s \langle v^2 \rangle - \frac{|\vec{I}|}{\rho c}}{\sigma_s - \sigma_a} \tag{11}$$

and

$$\langle v_s^2 \rangle = \frac{\sigma_a \langle v^2 \rangle - \frac{|\vec{I}|}{\rho c}}{\sigma_a - \sigma_s} \tag{12}$$

Substituting equations (11) and (12), respectively, into equation (1) gives

$$\Pi_a = \sigma_a \rho c \left(\frac{\sigma_s \langle v^2 \rangle - \frac{|\vec{I}|}{\rho c}}{\sigma_s - \sigma_a} \right) S \tag{13}$$

and

$$\Pi_s = \sigma_s \rho c \left(\frac{\sigma_a \langle v^2 \rangle - \frac{|\vec{I}|}{\rho c}}{\sigma_a - \sigma_s} \right) S \tag{14}$$

Equations (13) and (14) suggest that measurable differences in radiation efficiencies for airborne and structureborne noise permit the separation and prediction of the airborne and structureborne components of the total sound power radiated by some unknown combination of acoustic and vibrational inputs to a thin-shell structure.

EQUIPMENT AND PROCEDURES

Instrumentation

The instrumentation system used for the measurements was a combination of a two-microphone, cross-spectral, acoustic intensity probe for the measurement of space-time averaged intensity and an array of miniature, piezoelectric accelerometers for measuring the space-averaged, mean-square surface velocity of the structure. This instrumentation system is shown in figure 1. A 50-mm spacing between microphone center axes of two 1.252-cm-diameter microphones was used for the two-microphone, cross-spectral, acoustic intensity probe. This microphone spacing provided an accurate measurement of intensity in the frequency range from 100 to 1000 Hz. The two-microphone method uses the following equation to calculate acoustic intensity:

$$|\vec{I}| = \frac{Q_{12}}{\rho\omega\Delta r} \tag{15}$$

The array of accelerometers in figure 1 is used to calculate space-averaged, mean-square surface velocity by measuring the power spectrum of acceleration for each accelerometer signal, dividing each result by the square of the angular frequency to obtain the power spectrum of the velocity, and then averaging each of these results together to obtain a space average.

Measurement Facility

The measurement method was evaluated on several simple and built-up panels which were mounted in the transmission loss apparatus in the Langley Aircraft Noise Reduction Laboratory. The transmission loss (TL) apparatus consists of a source room and a receiving room. The two rooms have an adjoining wall that has a 1.23-m by 1.525-m porthole made for mounting simple panels and built-up aircraft panels between the two rooms. Figures 2 and 3 show sketches of the TL apparatus. Details on the geometry and on the acoustic properties of this facility are available in reference 34. Several large fiberglass panels were added to the receiving room to reduce the ambient noise level and to suppress any reactive components of the acoustic impedance (reflected waves) that the test panel might experience in the receiving space. The effectiveness of these fiberglass panels is discussed in reference 34.

Figure 2 shows how the TL apparatus was used to measure the airborne radiation efficiency of a test panel. Two independently driven loudspeakers, placed in the corners of the source room opposite the test panel, were used as a purely acoustic input to the test panel. This speaker arrangement produces a diffuse acoustic field in the source room at frequencies above 200 Hz. (See ref. 34.) At frequencies below 200 Hz, the sound field in the source room is probably not diffuse because of the low modal density of the source room. A rotating microphone boom, shown in figure 2, was used to measure the space-time averaged sound-pressure level in the source room.

The data were averaged over 10 full rotations of the boom to ensure that an accurate representation of the sound field in the source room was obtained.

Figure 3 shows how the TL apparatus was used to measure the structureborne radiation efficiency of a test panel. A 44.5 N peak-force vibration shaker was suspended from the wall of the source room by means of a cord and was attached to the test panel as shown in figure 3. The shaker and the test panel were coupled by using a force gage so that the power spectrum of the input force could be measured. The noise produced by the shaker was considered negligible since the sound pressure level in the source room that is produced by the shaker is at least 60 dB or more below the sound pressure level in the source room produced by the speaker system. (See fig. 2.)

Test Panels

Three basic panel designs were tested with the new measurement method for separating airborne and structureborne sound power. Since these tests were the first using the new measurement method, and since the purpose was to determine the accuracy and limitations of the method, the radiative properties of the test panels were of the secondary consideration. Consequently, the tests were restricted to a 929-cm^2 area in the center of each panel. By restricting the tests to this small area, the measurement time was significantly reduced. (The area chosen for the analysis must be large enough to obtain a meaningful space average.) Figure 4 shows a sketch of the 929-cm^2 area that was investigated on each on the three panels and also shows the shaker driving-point location on the source-room side of the panel.

A brief description of each of the three panel designs is given as follows:

Panel 1: The first panel was a 0.0813-cm-thick sheet of 2024 aluminum alloy. This simple aluminum sheet is made of the same material that is commonly used for the skin in the construction of aircraft fuselages. The coincidence frequency of this aluminum sheet is approximately 16 000 Hz.

Panel 2: The second panel was a skin-stiffened aluminum panel. A sketch of the panel, as viewed from the receiving room, is shown in figure 5. The panel has a 0.0813-cm-thick aluminum skin with 4 vertical frames and 10 horizontal stringers. Components of the panel were fabricated according to the practices of general aviation fuselage design.

Panel 3: The third panel was a duplicate of the second panel and was tested with the addition of a commercially available sound-damping tape. The self-adhesive damping tape was applied so that the entire surface of the receiving-room side of the panel was covered. The stringers and frames of the panel were left untreated (exposed).

Measurement and Analysis Procedure

The measurement and analysis procedure on each of the three test panels is described as follows:

(1) (a) The speakers in the source room were driven independently by two broadband white-noise generators; and the space-time averaged acoustic intensity which was transmitted through the test area on the panel, was measured by using the two-microphone intensity probe as shown in figure 2.

(b) The shaker system in the source room was driven by a broadband white-noise generator; and the space-time averaged acoustic intensity, which was radiated by the test area on the panel, was measured by using the two-microphone intensity probe as shown in figure 3.

Both sets of intensity data were stored for later use.

(2) (a) With the speakers driven as before, the space-averaged, mean-square surface acceleration of the test area on the panel was measured by using an array of miniature (2-gram) accelerometers. Data were obtained and stored for a total of 18 different accelerometer locations. The sampling distribution was random so that the measurements could be averaged together without bias toward any particular flexural mode shape of the test panel.

(b) With the shaker in the source room driven as before, the space-averaged, mean-square acceleration of the test area on the panel was measured by using the array of accelerometers. The same random distribution of 18 accelerometer locations was used.

The mean-square acceleration data obtained from these measurements were stored and later converted to mean-square velocity data, and then they were averaged together for the two cases of purely acoustic and purely vibrational inputs.

(3) The acoustic intensity data obtained in step 1 and the mean-square velocity data obtained in step 2 were used in conjunction with equation (2) to calculate the airborne and structureborne radiation efficiencies of the 929-cm^2 area on the test panel as a function of frequency.

(4) The test panel was then simultaneously subjected to some unknown combination of acoustic and vibrational inputs of interest and -

(a) The space-time averaged acoustic intensity radiated by the test area was measured by using the intensity probe.

(b) The space-averaged, mean-square surface velocity on the test area was measured by using the array of accelerometers.

(c) The information obtained in steps 4(a) and 4(b) was then used in conjunction with the airborne and structureborne radiation-efficiency data, and equations (13) and (14) were used to separate and predict the fractional amount of the total sound power radiated that was attributable to the airborne and structureborne paths.

(5) These airborne and structureborne sound-power predictions were then verified by -

(a) Measuring the sound power radiated by the test area with the speakers acting alone and then comparing the measurement with the sound power predicted by equation (13).

(b) Measuring the sound power radiated by the test area with the shaker acting alone and then comparing the measurement with the sound power predicted by equation (14).

MEASUREMENT RESULTS

Two independent sets of measurements were performed on each test panel. The first set of measurements was made by using incoherent acoustic and vibrational inputs (with the speakers and shaker driven by independent broadband noise generators). The second set of measurements was made by using coherent acoustic and vibrational inputs (with the speakers and shaker driven by a single broadband noise generator). The results presented in this paper are restricted to the case of fully coherent inputs since it is considered more indicative of the general case of multiple-input problems.

The results of the measurements on the three panels are given in figures 6 to 22. The bandwidth of the spectra in each of these figures is 2.5 Hz. Radiation-efficiency data and sound-power-level data (occasionally referred to as noise in the figures) for the panels are plotted over the frequency range from 100 to 1000 Hz. Sound-power-level data in the frequency range from 0 to 100 Hz, although available, were not plotted since the data in that range may be inaccurate. (The two-microphone, cross-spectral method of acoustic intensity measurement suffers from phase-shift errors at low frequency. See refs. 12 to 17 and 27 to 30 for details on the limitations of this measurement method.)

Aluminum Sheet (Panel 1)

The measurement results on the simple aluminum sheet (panel 1) are presented in figures 6 to 12. Figure 6 shows the measured airborne and structureborne radiation efficiencies of the aluminum sheet. This figure shows that a marked, measurable difference in airborne and structureborne radiation efficiencies exists in the frequency range from 100 to 1000 Hz. These two radiation-efficiency curves were used in conjunction with equations (13) and (14) for all subsequent airborne and structureborne sound-power predictions on panel 1.

A series of airborne and structureborne sound-power predictions were performed by using the coherent, simultaneous acoustic and vibrational inputs shown in figures 7 and 8. The total composite sound power radiated by the 929-cm^2 area of the panel was measured as outlined in preceding sections of this paper. Comparisons of this measured composite sound power with the airborne sound power predicted by equation (13) and with the structureborne sound power predicted by equation (14) are shown in figures 9 and 10, respectively. These two figures suggest that the airborne noise is dominant in the frequency range from 600 to 1000 Hz, the structureborne noise is dominant in the frequency range from 100 to 350 Hz, and the airborne and structureborne noise components are equally important in the frequency range from 350 to 600 Hz.

The predictions shown in figures 9 and 10 are verified in figures 11 and 12. The comparison of actual (measured) and predicted airborne noise, given in figure 11, shows that the prediction approach of equation (13) does quite well when the airborne sound power is the dominant source of noise. The airborne sound-power level is slightly overestimated, however, when the airborne component is not the dominant source of noise. The comparison of actual (measured) and predicted structureborne noise, given in figure 12, indicates that the prediction approach of equation (14) produces quite accurate results over the entire frequency range.

Aircraft Panel (Panel 2)

The measurement results on the built-up aircraft panel (panel 2) are presented in figures 13 to 17. Figure 13 shows the measured airborne and structureborne radiation efficiencies of the panel. The radiation-efficiency curves shown in this figure intersect at some frequencies. At those frequencies, equations (13) and (14) are inadequate for separating the airborne and structureborne sound-power components radiated by the panel since the equations have a singularity condition when the airborne and structureborne radiation efficiencies are equal.

Tests on the built-up aircraft panel were performed by using simultaneous, fully coherent, acoustic and vibrational inputs similar to the inputs shown in figures 7 and 8. Comparisons of the total composite sound power radiated by the 929-cm^2 area of the panel with the predicted airborne and structureborne sound-power components are shown in figures 14 and 15, respectively. Figure 14 indicates that the airborne noise is dominant in the frequency range from 400 to 1000 Hz, whereas figure 15 suggests that the structureborne noise is dominant below 400 Hz. If less than a 0.0001 difference existed between the airborne and structureborne radiation efficiencies at a particular frequency, all the composite sound power at that frequency was attributed to the acoustic source when predicting airborne sound power; and, similarly, all the composite sound power at that frequency was also attributed to the vibrational source when predicting the structureborne sound power. Since the radiation-efficiency curves for the built-up aircraft panel cross over at several points (e.g., around 630 Hz), there were several frequencies where all the composite noise was attributed to both the acoustic and the vibrational sources. The airborne and structureborne sound-power predictions at these frequencies then represent "worst case" conditions.

The predictions given in figures 14 and 15 are verified in figures 16 and 17, respectively. The comparisons between actual (measured) and predicted airborne and structureborne sound power given in figures 14 and 15 show that the predictions of equations (13) and (14) are not as accurate for built-up aircraft structures as they are for simple sheets of aluminum. According to the results given in these figures, however, the sound-power predictions are fully adequate for qualitatively determining which "peaks" in the composite sound-power spectrum are airborne in origin and which "peaks" are structureborne in origin.

Aircraft Panel With Damping Tape (Panel 3)

The measurement results on the built-up aircraft panel with damping tape added (panel 3) are presented in figures 18 to 22. Figure 18 shows the measured airborne and structureborne radiation efficiencies of the panel. A comparison of these radiation-efficiency curves (panel 3) with the radiation-efficiency curves of the plain aircraft panel (panel 2) shown in figure 13 clearly demonstrates the effects of added damping. In contrast with the plain built-up aircraft panel, the aircraft panel with added damping exhibits a very large difference in its airborne and structureborne radiation efficiencies. A close comparison of figures 13 and 18 also reveals that the radiation-efficiency curves of the damped aircraft panel are much "smoother" than the radiation-efficiency curves of the plain aircraft panel.

Tests on the damped aircraft panel were performed by using simultaneous, fully coherent acoustic and vibrational inputs, similar to the inputs shown in figures 7 and 8. Comparisons of the total composite sound power radiated by the 929-cm^2 area on the panel with the predicted airborne and structureborne sound-power components

are shown in figures 19 and 20, respectively. These figures show that the airborne noise is dominant over most of the frequency range from 100 to 1000 Hz, whereas the structureborne noise is dominant only below 200 Hz.

The sound-power predictions presented in figures 19 and 20 are verified in figures 21 and 22, respectively. The comparisons of actual (measured) and predicted airborne and structureborne sound powers given in figures 21 and 22 indicate that the predictions of equations (13) and (14) produce slightly more accurate results for the damped aircraft panel than for the undamped aircraft panel.

DISCUSSION

Limitations of Measurement Method

The first, and most obvious, limitation of this new noise–path separation method is its low-frequency restriction. Since there is little or no difference in airborne and structureborne radiation efficiencies above coincidence, the method can be used only in the frequency range below the coincidence frequency of the structure.

A second limitation of the method stems from the uncertainties introduced by the sources used for the radiation-efficiency measurements. Idealized sources such as loudspeakers and shakers may not be adequate representations of purely acoustic and purely vibrational inputs for some practical problems of interest. For example, suppose a loudspeaker is used as an acoustic source to determine the airborne radiation efficiency of some small area on a propeller-driven aircraft fuselage. The acoustic directivity of the loudspeaker may be dissimilar to the directivity of the actual acoustic sources on the aircraft (i.e., the propellers). Changes in acoustic source directivity can alter the effective airborne radiation efficiency measured for the structure. The hydrodynamic loading on the fuselage caused by the propellers could also change the airborne radiation efficiency to some degree.

Similarly, if the shaker system used to calibrate the structure does not produce a vibrational input with transmission paths that adequately simulate the structural transmission paths of the actual vibrational sources on the airplane (viz, the engines), the actual structureborne radiation efficiency of the aircraft fuselage will probably differ from that which is measured. A complex structure such as a propeller-driven aircraft may have several important structural transmission paths. Measuring structureborne radiation efficiencies for many structural transmission paths would not necessarily solve the problem since the relative importance of the different structural paths may be unknown. (By measuring more than one structureborne radiation efficiency, eqs. (8) and (10) become a system of two equations and three unknowns, which cannot be solved unless the relative importance of the different structural paths is known.)

A third limitation of the measurement method arises when the airborne and structureborne radiation efficiencies are equal in some frequency range of interest. Under these conditions, a conservative approach is to attribute all the total composite sound power radiated to <u>both</u> the airborne and structureborne sound powers. This ensures that the sound-power predictions represent the "worst case." Another plausible alternative would be to alter the structure somehow so that there is a difference in the airborne and structureborne radiation efficiencies. The effectiveness of alterations in the structure was demonstrated by the large difference in airborne radiation efficiencies measured on panels 2 and 3. (Compare figs. 13 and 18.)

The fourth limitation of the method is the inaccuracies in the airborne and structureborne sound-power predictions that were evident in the measurement results of this study. The most noticeable of these inaccuracies was the consistent tendency of the airborne prediction to overestimate the airborne component at those frequencies where its contribution to the total composite noise is small compared with the structureborne contribution. Presently, it is not fully understood why this happens with the airborne sound-power predictions, whereas the structureborne sound-power predictions seem to remain accurate even in frequency ranges where the relative contribution of the structureborne noise is far below that of the airborne noise. Further research is needed before this new noise-path separation method can be applied to practical problems with confidence.

Advantages of Measurement Method

This new measurement method has several advantages over the other noise-path identification methods currently proposed. One of the alternate methods for separating airborne and structureborne noise in aircraft is to measure the noise levels in the cabin with the engines running normally and with the engines detached. The obvious limitation of this method is that the tests cannot be performed in flight. Detaching the engines may also prove to be a costly and impractical method for determining the relative importance of the structureborne noise for a diverse fleet of aircraft. The noise-path separation method proposed in this paper does not necessarily require modifications to the aircraft and, in principle, could be used during flight.

The measurement method also has advantages over the use of lead-wrapping methods and partial and/or multiple coherence function measurements. The measurement method can be used for fully coherent acoustic and vibrational inputs, whereas the partial and/or multiple coherence function method cannot. The measurement method works best in the low-frequency range where lead-wrapping methods fail because of the poor transmission loss of lead.

CONCLUDING REMARKS

The noise-path separation method proposed in this paper has been used successfully to predict the relative contributions of the airborne and structureborne sound-power components of arbitrarily chosen combinations of simultaneous acoustic and vibrational inputs for three different, distinct panel designs. The use of radiation-efficiency measurements for separating the airborne and structureborne components of the total radiated sound power of aircraft panels appears to be a viable option to the other diagnostic tools currently available. The results of the study indicate that the method is quick, reliable, and inexpensive, and it can be applied to thin-shell structures of various designs.

Langley Research Center
National Aeronautics and Space Administration
Hampton, VA 23665
August 26, 1982

REFERENCES

1. Catherines, John J.; and Mayes, William H.: Interior Noise Levels of Two Propeller-Driven Light Aircraft. NASA TM X-72716, 1975.

2. Catherines, John J.; and Jha, Sunil K.: Sources and Characteristics of Interior Noise in General Aviation Aircraft. NASA TM X-72839, 1976.

3. Jha, S. K.; and Catherines, J. J.: Interior Noise Studies for General Aviation Types of Aircraft, Part I: Field Studies. J. Sound & Vib., vol. 58, no. 3, June 8, 1978, pp. 375-390.

4. Unruh, James F.; and Scheidt, Dennis C.: Engine Induced Structural-Borne Noise in a General Aviation Aircraft. SAE Tech. Pap. Ser. 790626, Apr. 1979.

5. Unruh, James F.; Scheidt, Dennis C.; and Pomerening, Daniel J.: Engine Induced Structural-Borne Noise in a General Aviation Aircraft. NASA CR-159099, 1979.

6. Unruh, J. F.: Structural-Borne Noise Prediction for a Single Engine General Aviation Aircraft. AIAA-80-1037, June 1980.

7. Unruh, James F.; and Scheidt, Dennis C.: Engine Isolation for Structural-Borne Interior Noise Reduction in a General Aviation Aircraft. NASA CR-3427, 1981.

8. Jha, S. K.; and Catherines, J. J.: Interior Noise Studies for General Aviation Types of Aircraft, Part II: Laboratory Studies. J. Sound & Vib., vol. 58, no. 3, June 8, 1978, pp. 391-406.

9. Keefe, Laurence: Interior Noise Path Identification in Light Aircraft Using Multivariate Spectral Analysis. AIAA Paper 79-0644, Mar. 1979.

10. Howlett, James T.: A Study of Partial Coherence for Identifying Interior Noise Sources and Paths on General Aviation Aircraft. NASA TM-80197, 1979.

11. Bendat, Julius S.; and Piersol, Allan G.: Engineering Applications of Correlation and Spectral Analysis. John Wiley & Sons, Inc., c.1980.

12. Fahy, Frank J.: Measurement of Acoustic Intensity Using the Cross-Spectral Density of Two Microphone Signals. J. Acoust. Soc. America, vol. 62, no. 4., Oct. 1977, pp. 1057-1059.

13. Lambrich, H. P.; and Stahel, W. A.: A Sound Intensity Meter and Its Applications in Car Acoustics. INTER-NOISE 77 Proceedings - Noise Control: The Engineer's Responsibility, Eric J. Rathe, ed., c.1977, pp. B 142 - B 147.

14. Chung, J. Y.: Fundamental Aspects of the Cross-Spectral Method of Measuring Acoustic Intensity. Progrès Récents Dans la Mesure de l'Intensité Acoustique (Recent Developments in Acoustic Intensity Measurement), Cent. Tech. Ind. Mec., c.1981, pp. 1-10.

15. Lyon, Richard H.: DD6. Some Observations on Sound Intensity Measurements. Program of the 99th Meeting. J. Acoust. Soc. America, vol. 67, suppl. 1, Spring 1980, p. S70.

16. Thompson, J. K.; and Tree, D. R.: Finite Difference Approximation Errors in Acoustic Intensity Measurements. J. Sound & Vib., vol. 75, no. 2, Mar. 22, 1981, pp. 229-238.

17. Seybert, A. F.: Statistical Errors in Acoustic Intensity Measurements. J. Sound & Vib., vol. 75, no. 4, Apr. 22, 1981, pp. 519-526.

18. Macadam, J.: The Measurement of Sound Radiation From Room Surfaces in Lightweight Buildings. Appl. Acoust., vol. 9, no. 2, April 1976, pp. 103-118.

19. Czarnecki, Stefan; Engel, Zbigniw; and Panuszka, Ryszard: Correlation Method of Measurements of Sound Power in the Near-Field Conditions. Arch. Acoust., vol. 1, no. 3, 1976, pp. 201-213.

20. Hodgson, Thomas H.: Investigation of the Surface Acoustical Intensity Method for Determining the Noise Sound Power of a Large Machine In Situ. J. Acoust. Soc. America, vol. 61, no. 2, Feb. 1977, pp. 487-493.

21. Brito, Jose Daniel: Sound Intensity Patterns for Vibrating Surfaces. Ph. D. Thesis, Massachusetts Inst. Technol., 1977.

22. McGary, Michael C.: Noise Source Identification of Diesel Engines Using Surface Intensity Measurement. M.S. Thesis, Purdue Univ., 1980.

23. Boone, Diane E.; and Hodgson, Thomas H.: Surface Intensity Measurements Using a Fiber Optic-Pressure Probe. Recent Developments in Acoustic Intensity Measurement, Cent. Tech. Ind. Mec., c.1981, pp. 89-94.

24. Williams, Earl G.; Maynard, J. D.; and Skudrzyk, Eugen: Sound Source Reconstructions Using a Microphone Array. J. Acoust. Soc. America, vol. 68, no. 1, July 1980, pp. 340-344.

25. Williams, Earl G.; and Maynard, Julian D.: Intensity Vector Field Mapping With Nearfield Holography. Recent Developments in Acoustic Intensity Measurement, Cent. Tech. Ind. Mec., c.1981, pp. 31-36.

26. Maynard, J. D.; and Williams, E. G.: Nearfield Holography, a New Technique for Noise Radiation Measurement. NOISE-CON 81 Proceedings - Applied Noise Control Technology, Larry H. Royster, Franklin D. Hart, and Noral D. Stewart, eds., c.1981, pp. 19-24.

27. Crocker, Malcolm J.; Forssen, Bjorn; Raju, P. K.; and Mielnicka, Anna: Measurement of Transmission Loss of Panels by an Acoustic Intensity Technique. INTER-NOISE 80 Proceedings - Noise Control for the 80's, Volume II, George C. Maling, Jr., ed., c.1980, pp. 741-746.

28. McGary, Michael C.: Interior Noise Source/Path Identification on Propeller-Driven Aircraft Using Acoustic Intensity Methods. NOISE-CON 81 Proceedings - Applied Noise Control Technology, Larry H. Royster, Franklin D. Hart, and Noral D. Stewart, eds., c.1981, pp. 261-264.

29. Crocker, Malcolm J.; Raju, P. K.; and Forssen, Bjorn: Measurement of Transmission Loss of Panels by the Direct Determination of Transmitted Acoustic Intensity. Noise Contr. Eng., vol. 17, no. 1, July-Aug. 1981, pp. 6-11.

30. McGary Michael C.: Noise Transmission Loss of Aircraft Panels Using Acoustic Intensity Methods. NASA TP-2046, 1982.

31. Vér, István L.; and Holmer, Curtis I.: Interaction of Sound Waves With Solid Structures. Noise and Vibration Control, Leo L. Beranek, ed., McGraw-Hill Book Co., c.1971, pp. 270-361.

32. Manning, Jerome E.; and Maidanik, Gideon: Radiation Properties of Cylindrical Shells. J. Acoust. Soc. America, vol. 36, no. 9, Sept. 1964, pp. 1691-1698.

33. Forssen, Bjorn; and Crocker, Malcolm J.: Estimation of Surface Velocity by Use of the Two Microphone Technique. INTER-NOISE 82 Proceedings - Noise Control: Ten Years Later, Volume II, James G. Seebold, ed., c.1982, pp. 687-690.

34. McGary, Michael C.: Sound Field Diffusivity in NASA Langley Research Center Hardwalled Acoustic Facilities. NASA TM-83275, 1982.

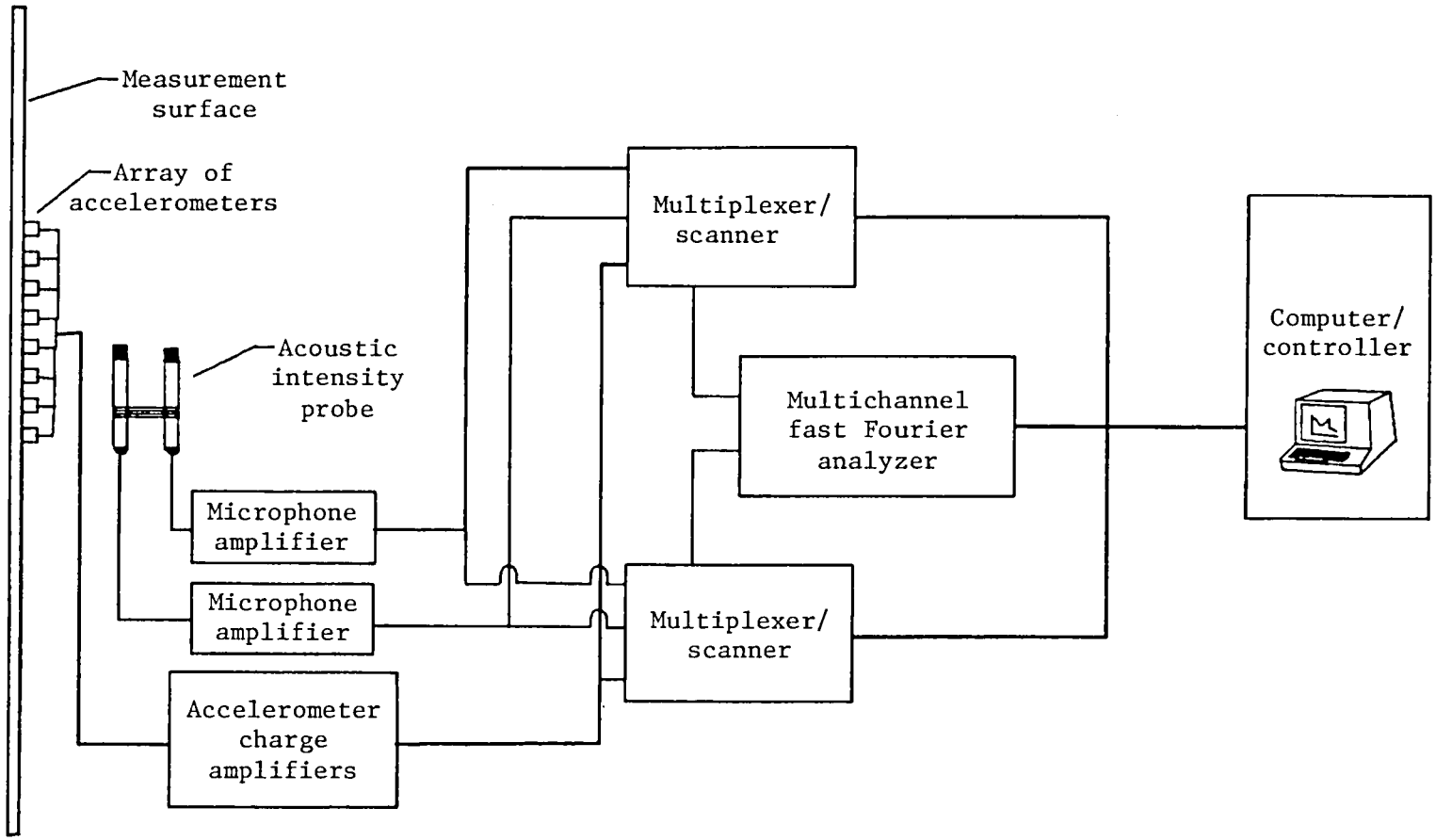

Figure 1.- Block diagram of instrumentation.

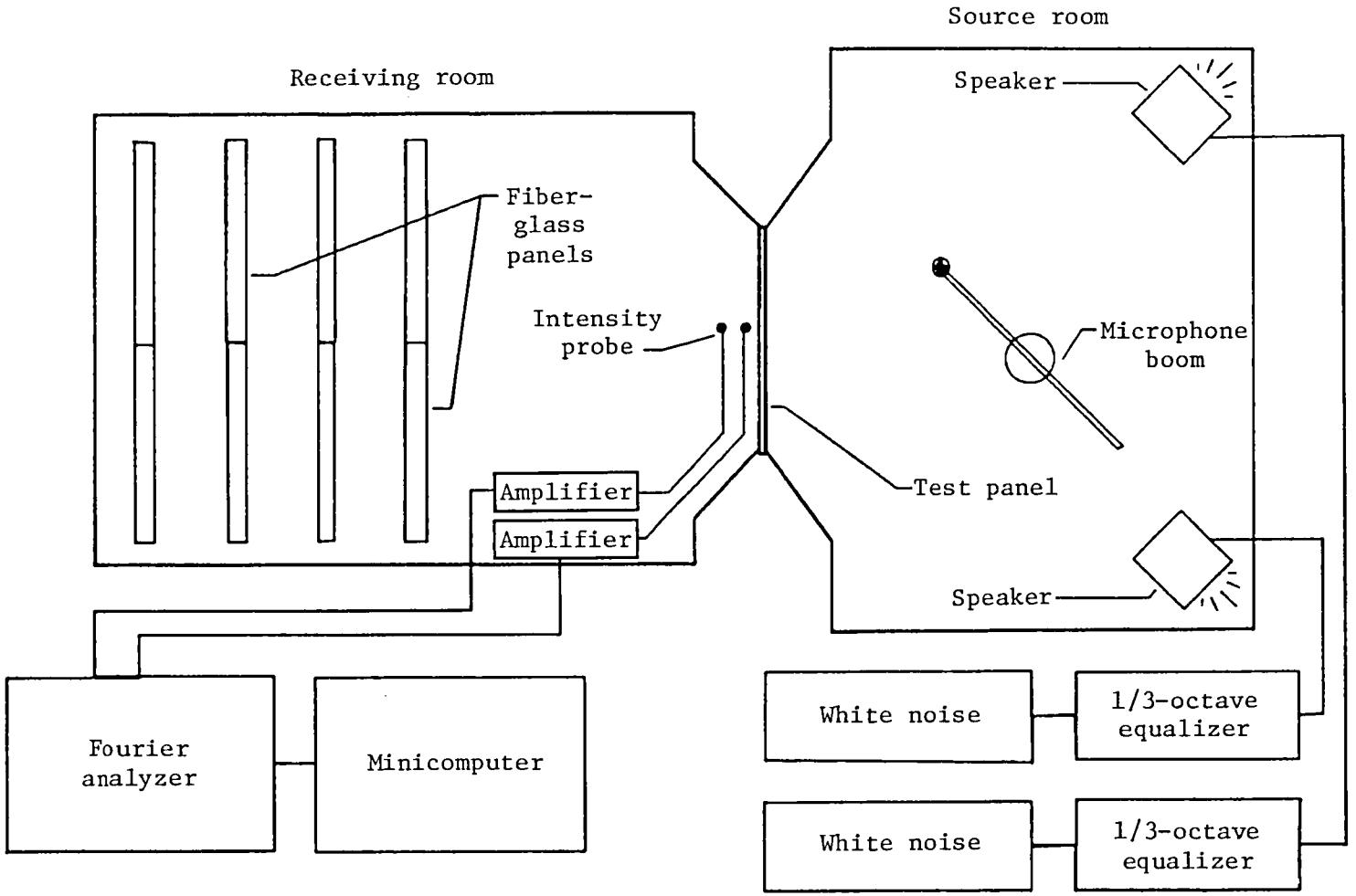

Figure 2.- Instrumentation in the transmission loss apparatus used to measure sound power radiated by a test panel excited by an acoustic input.

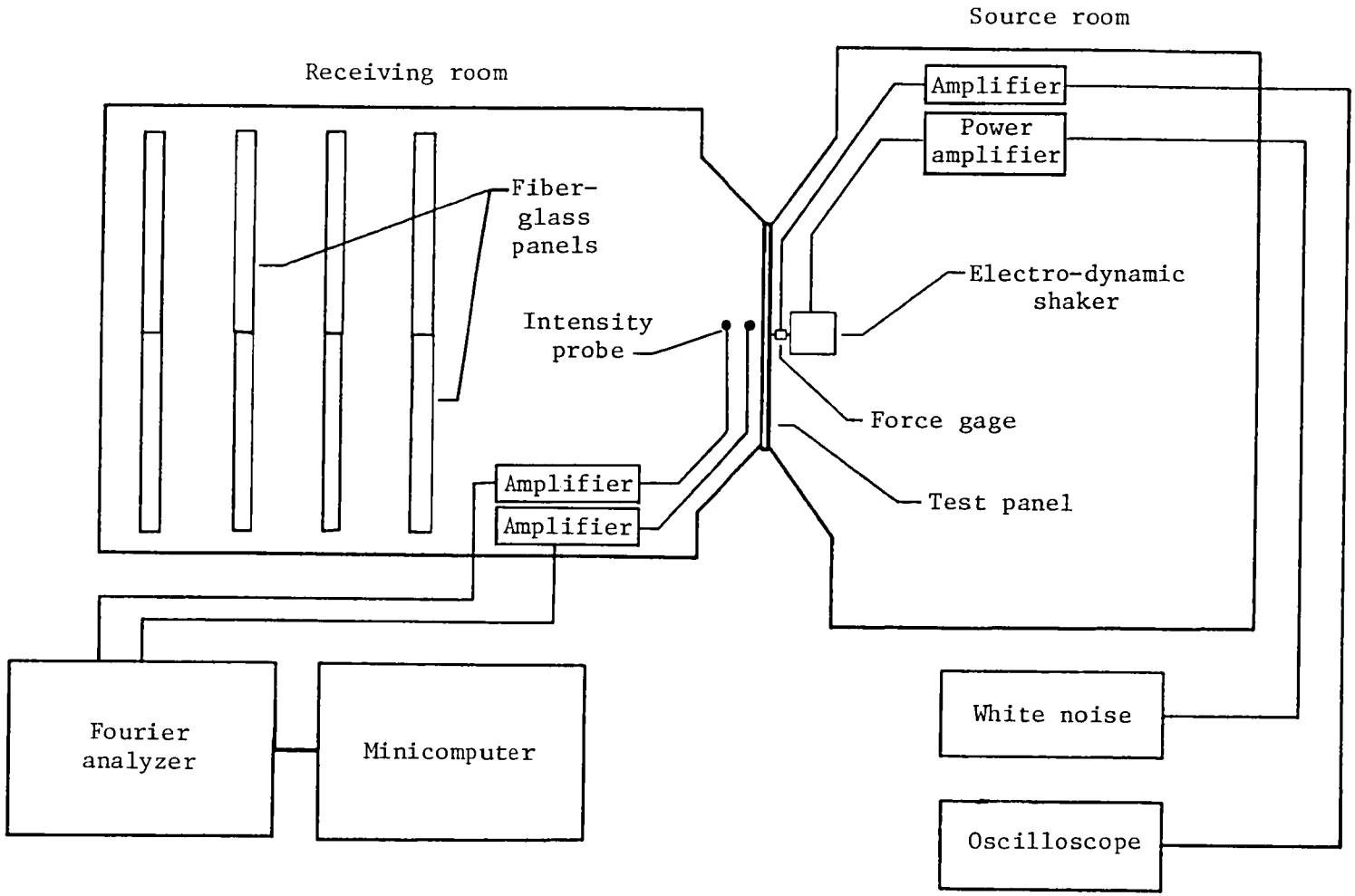

Figure 3.- Instrumentation in the transmission loss apparatus used to measure sound power radiated by a test panel excited by a vibrational input.

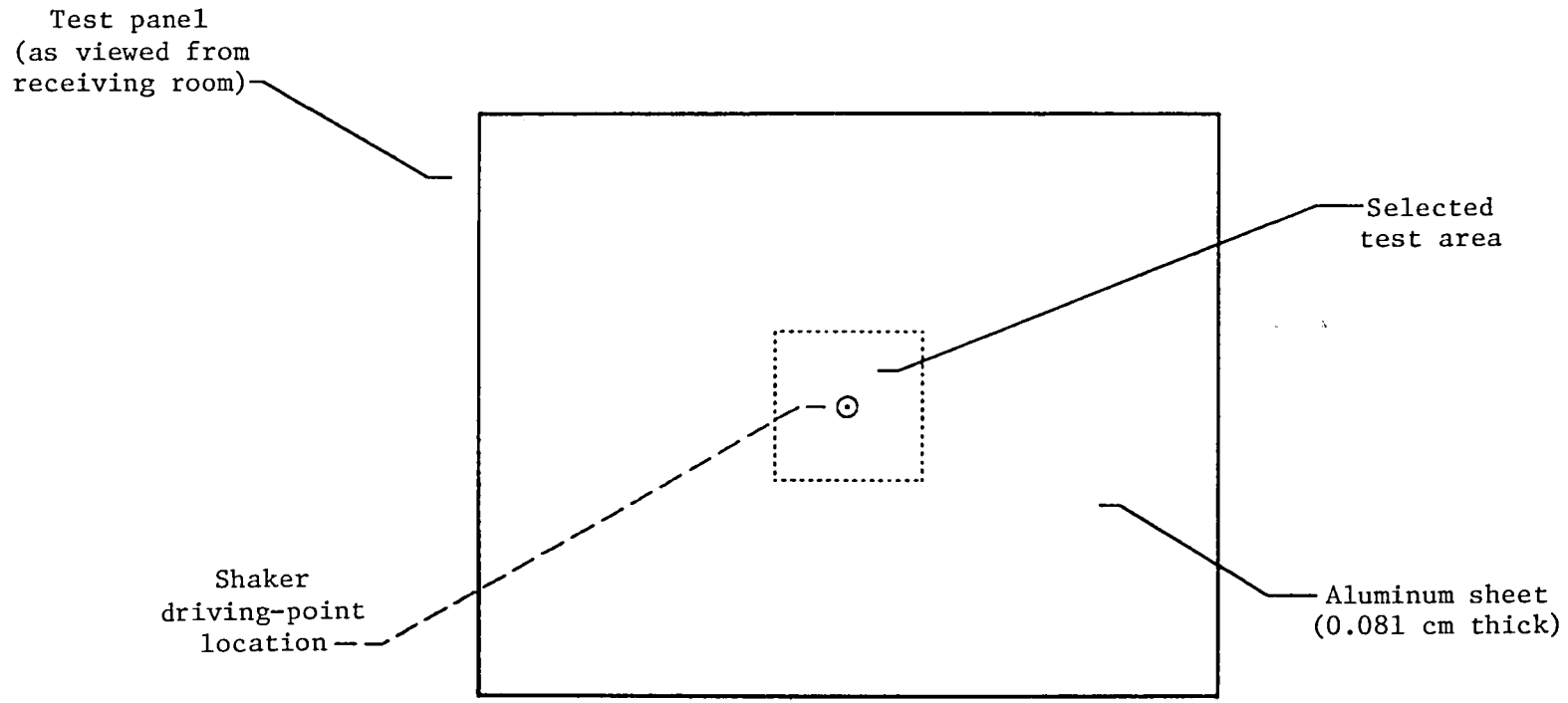

Figure 4.- Sketch of the 929-cm^2 test area.

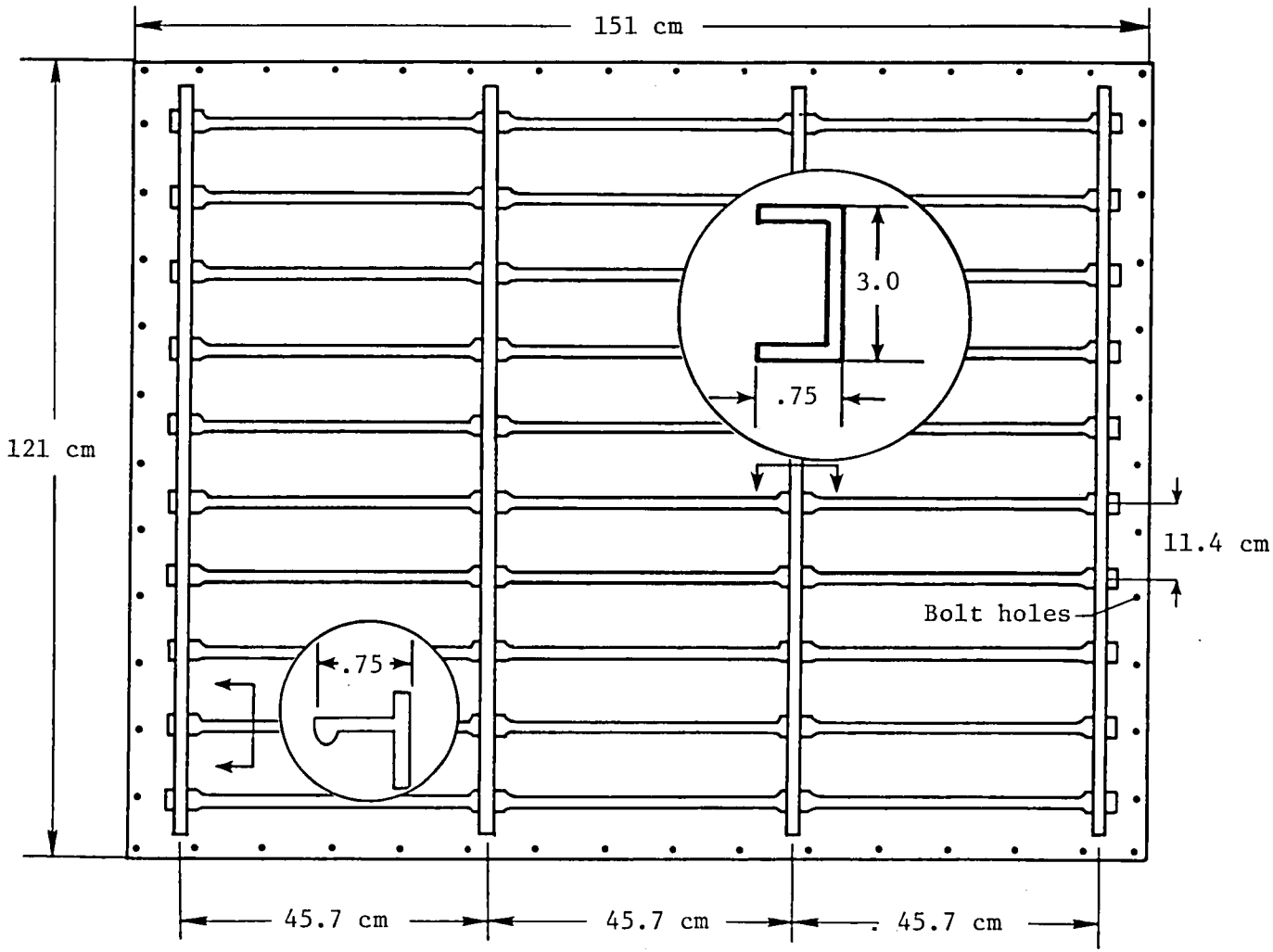

Figure 5.- Skin-stiffened aluminum panel. Panels 2 and 3.

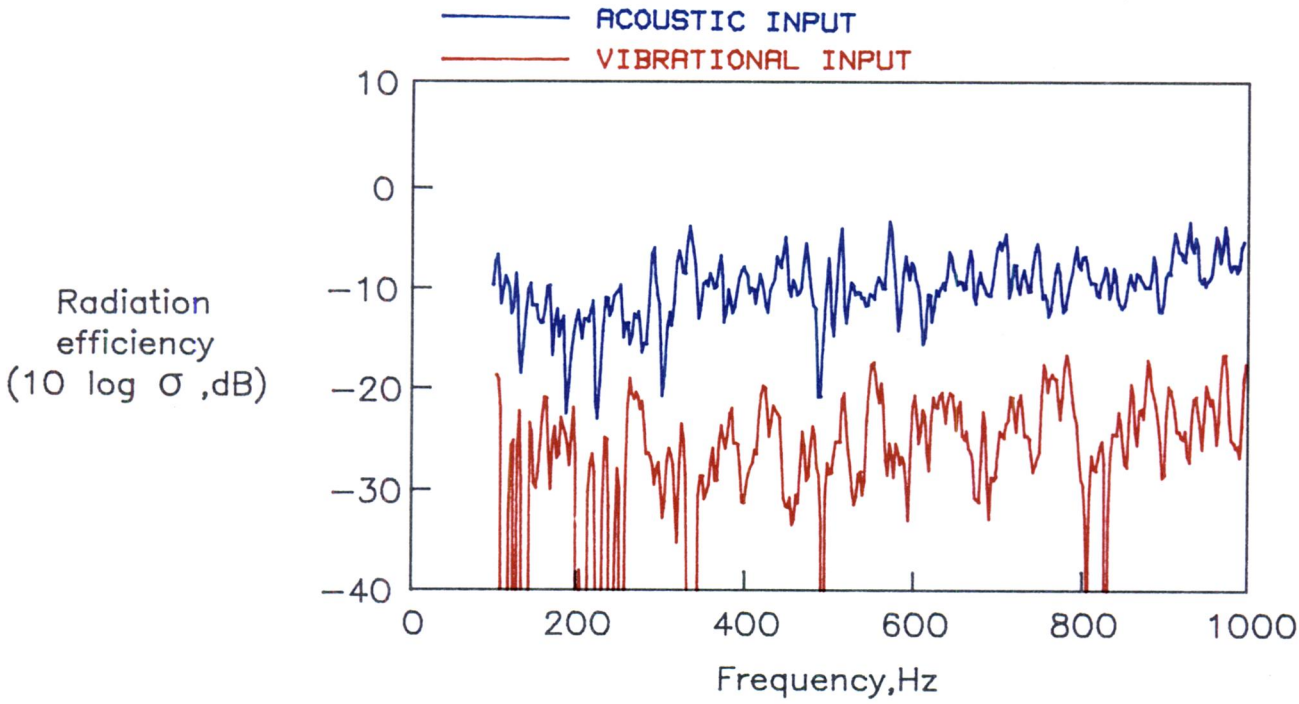

Figure 6.- Measured airborne and structureborne radiation efficiencies of the aluminum sheet. Panel 1.

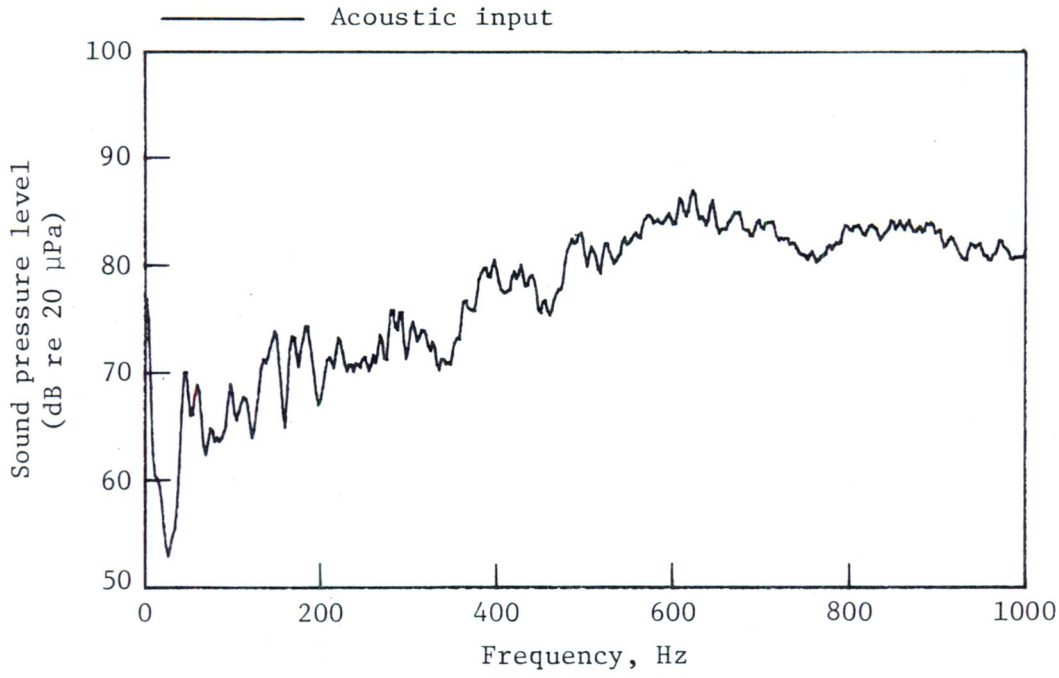

Figure 7.- Sound pressure level in source room for the coherent acoustic input to the aluminum sheet. Panel 1.

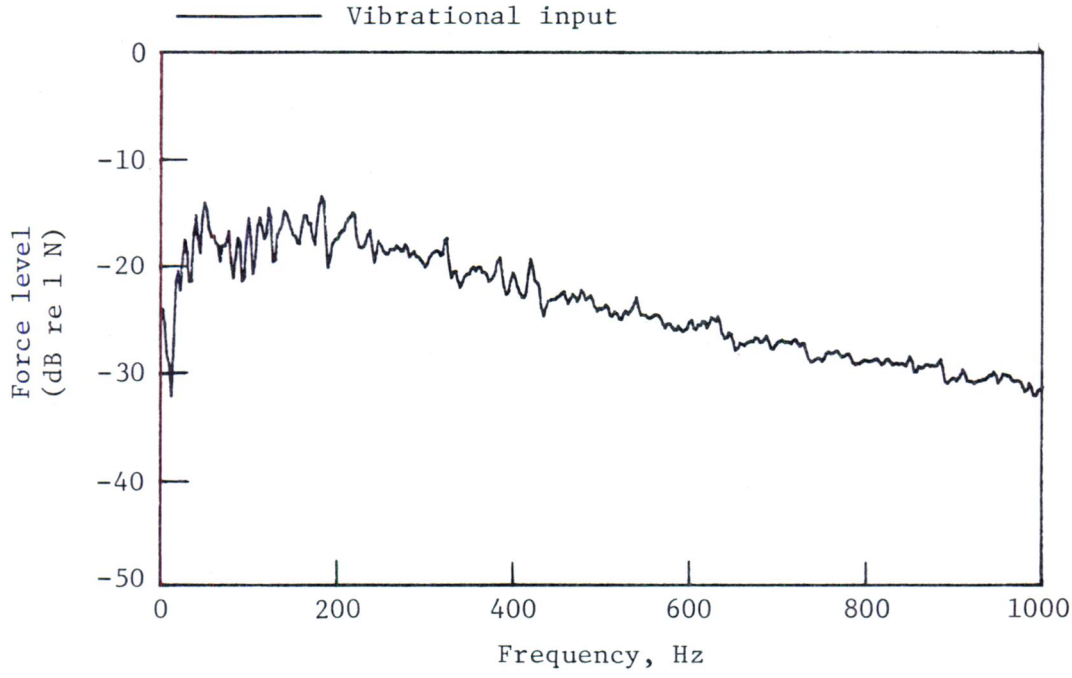

Figure 8.- Force-level input of shaker system for the coherent vibrational input to the aluminum sheet. Panel 1.

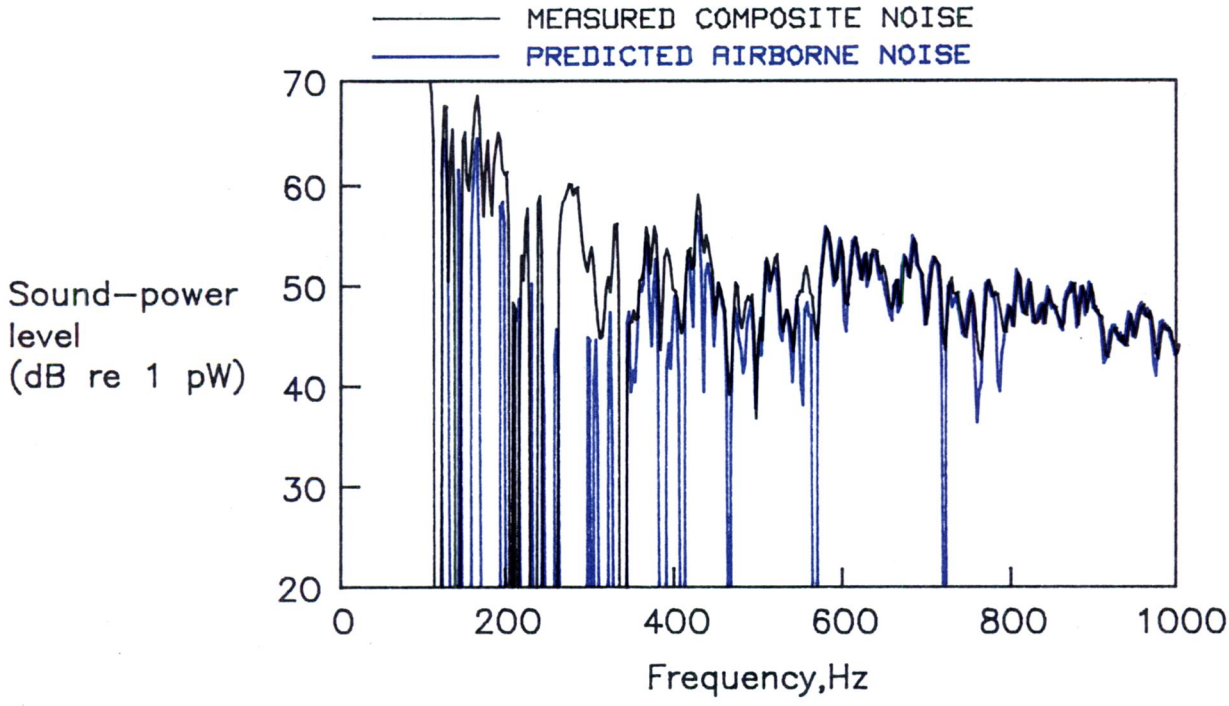

Figure 9.- Comparison of measured composite sound power and predicted airborne sound power for the aluminum sheet. Panel 1.

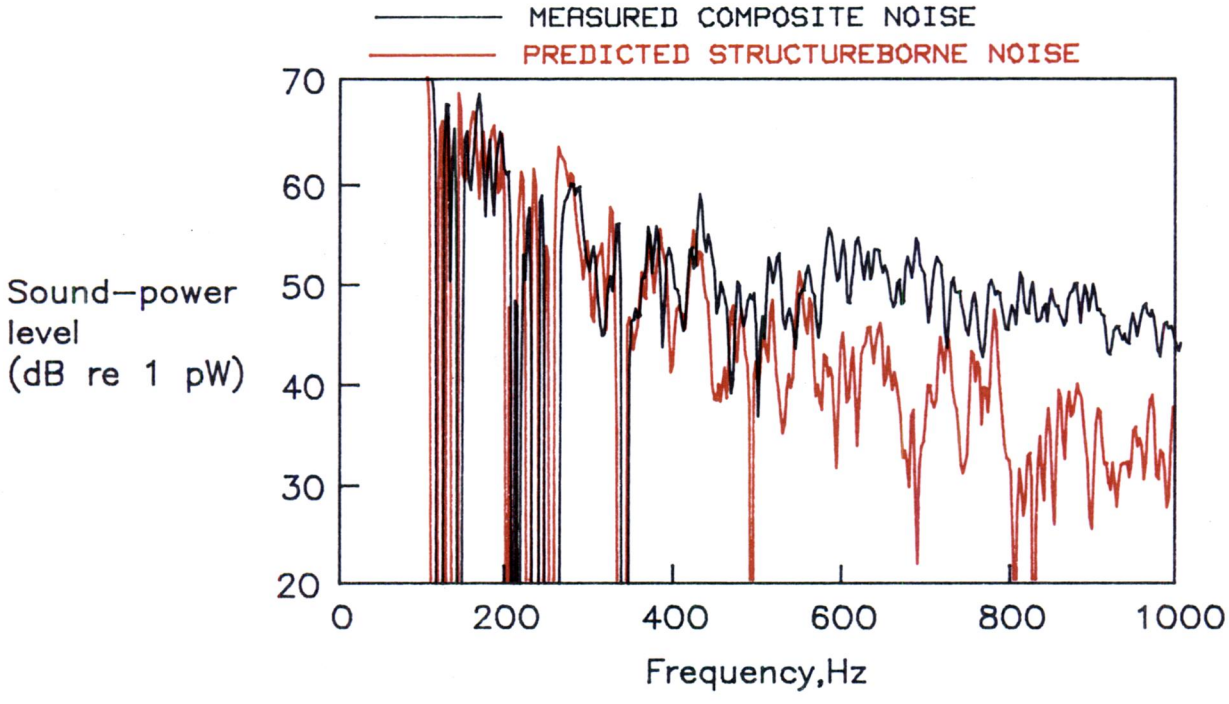

Figure 10.- Comparison of measured composite sound power and predicted structureborne sound power for the aluminum sheet. Panel 1.

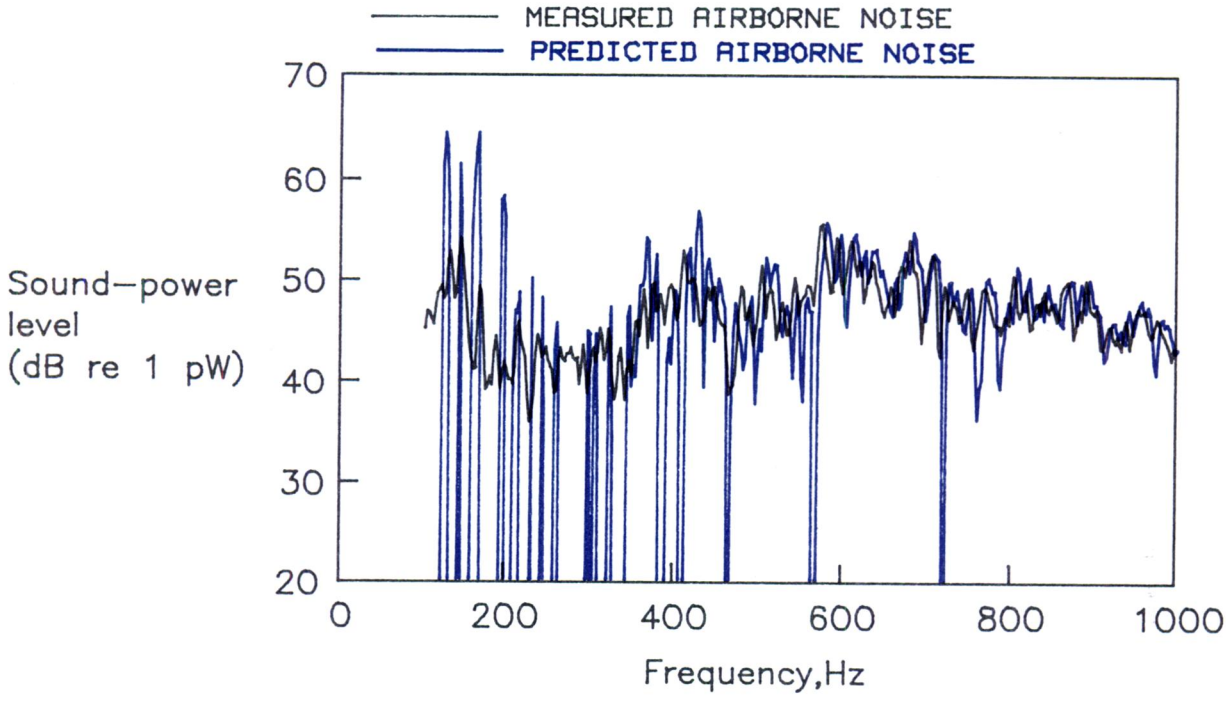

Figure 11.- Comparison of measured and predicted airborne sound powers for the aluminum sheet. Panel 1.

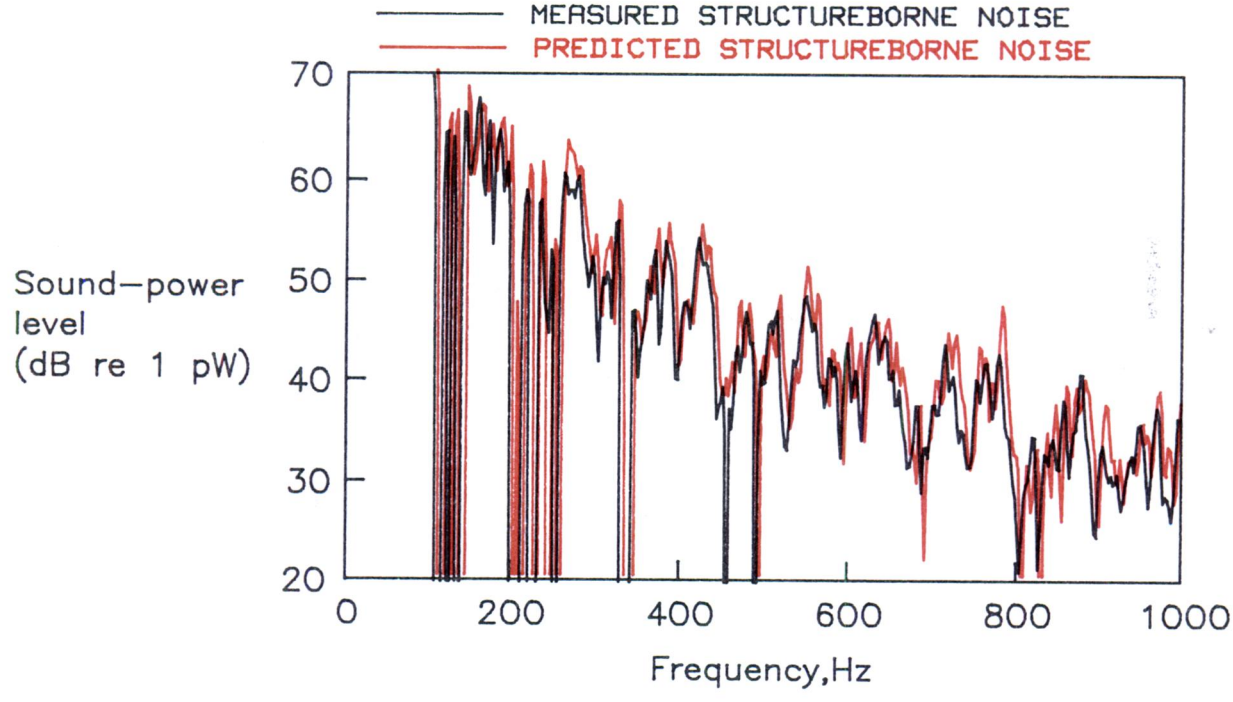

Figure 12.- Comparison of measured and predicted structureborne sound powers for the aluminum sheet. Panel 1.

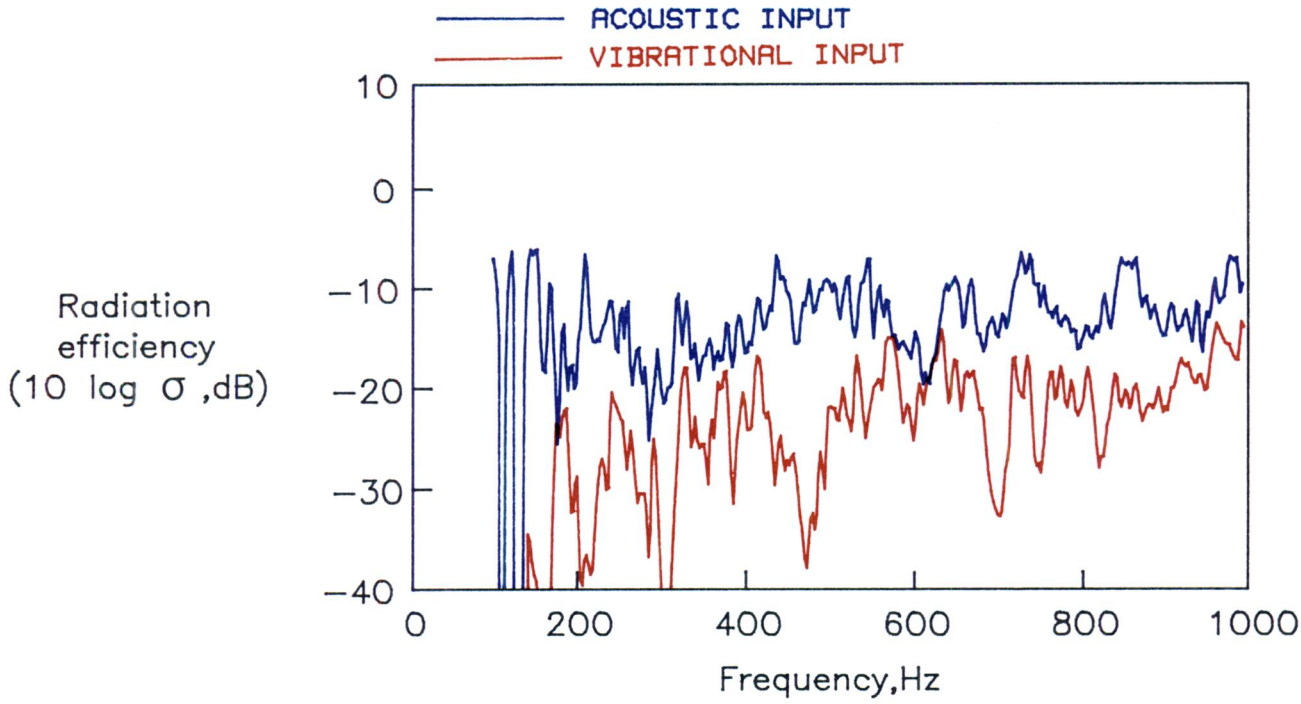

Figure 13.- Measured airborne and structureborne radiation efficiencies of the built-up aircraft panel. Panel 2.

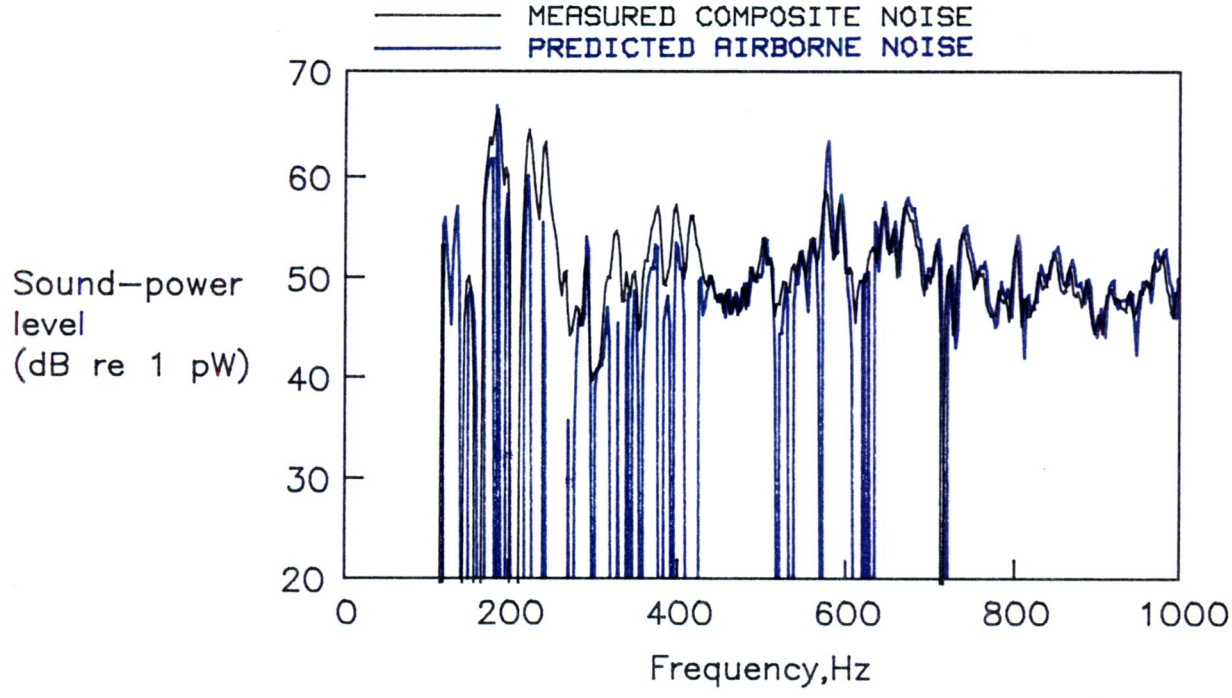

Figure 14.- Comparison of measured composite sound power and predicted airborne sound power for the built-up aircraft panel. Panel 2.

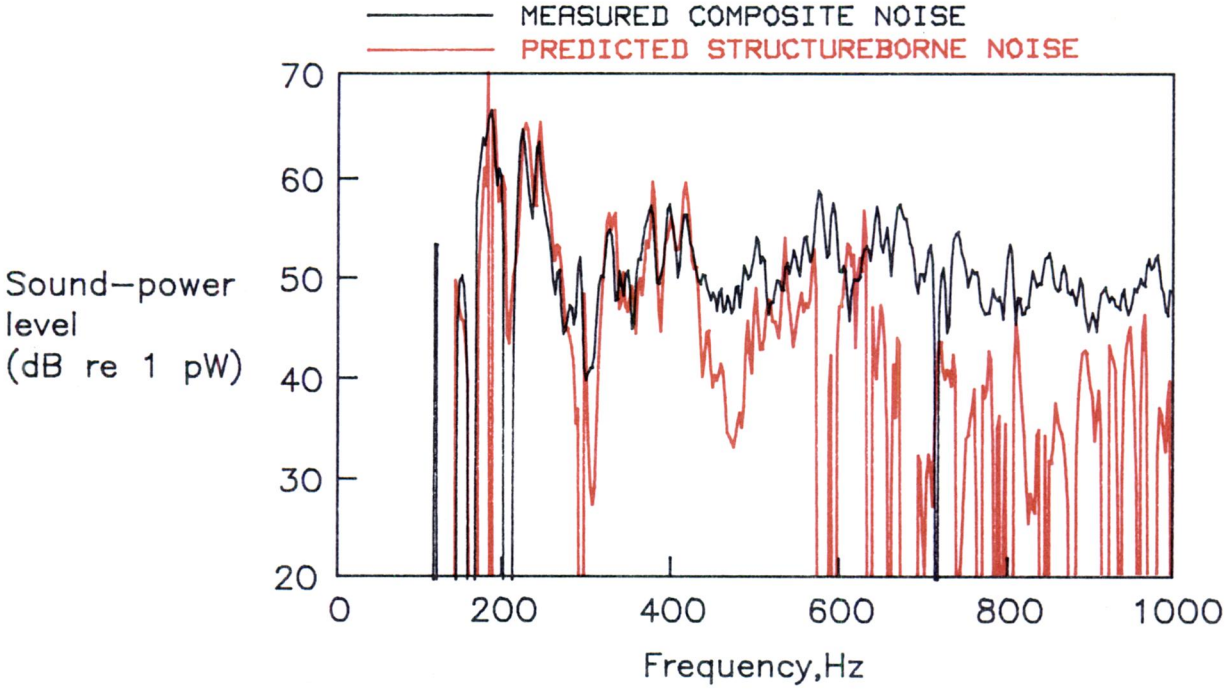

Figure 15.- Comparison of measured composite sound power and predicted structureborne sound power for the built-up aircraft panel. Panel 2.

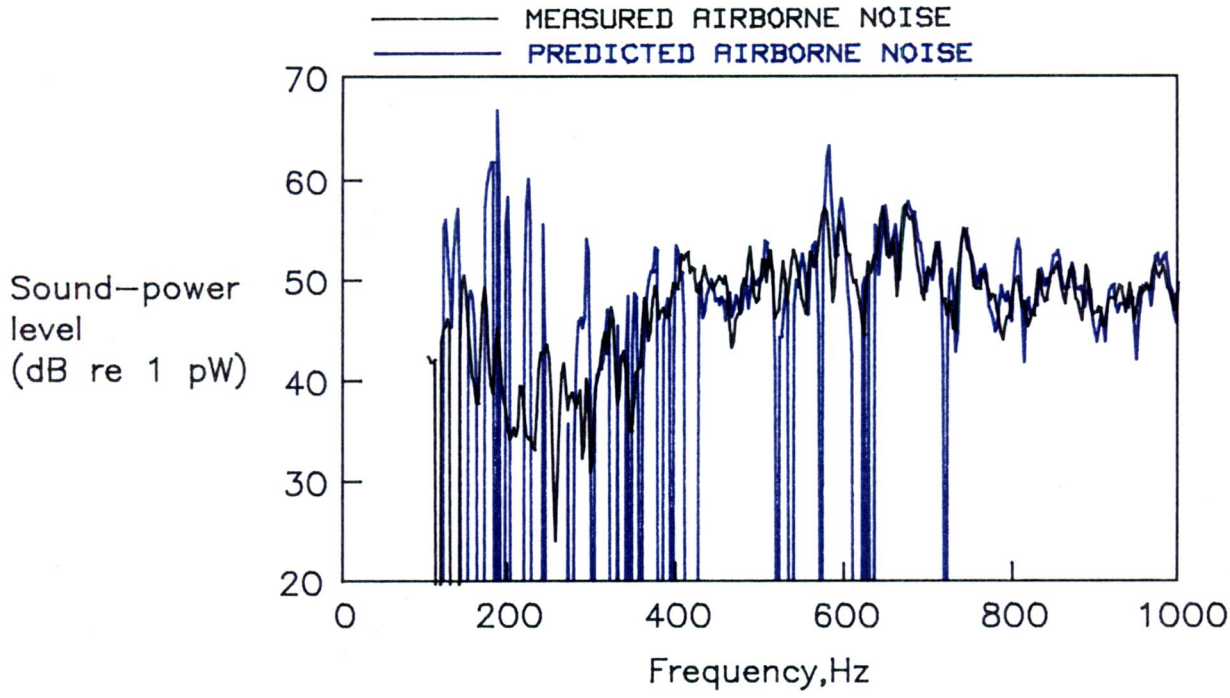

Figure 16.- Comparison of measured and predicted airborne sound powers for the built-up aircraft panel. Panel 2.

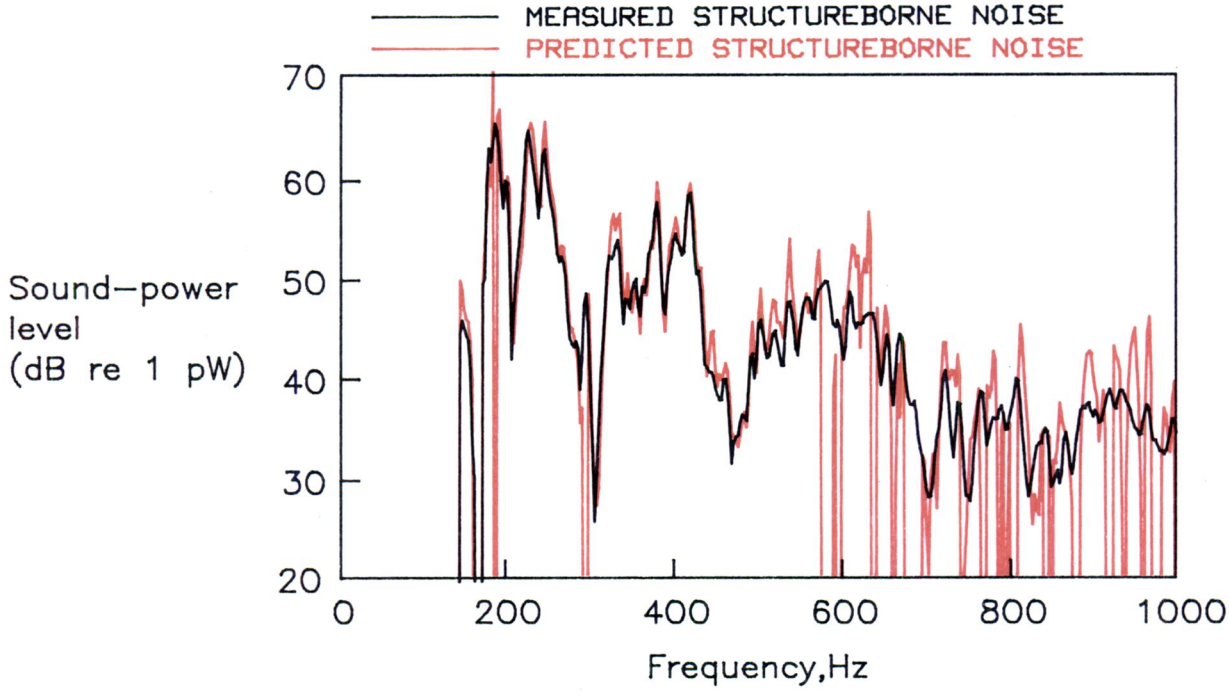

Figure 17.- Comparison of measured and predicted structureborne sound powers for the built-up aircraft panel. Panel 2.

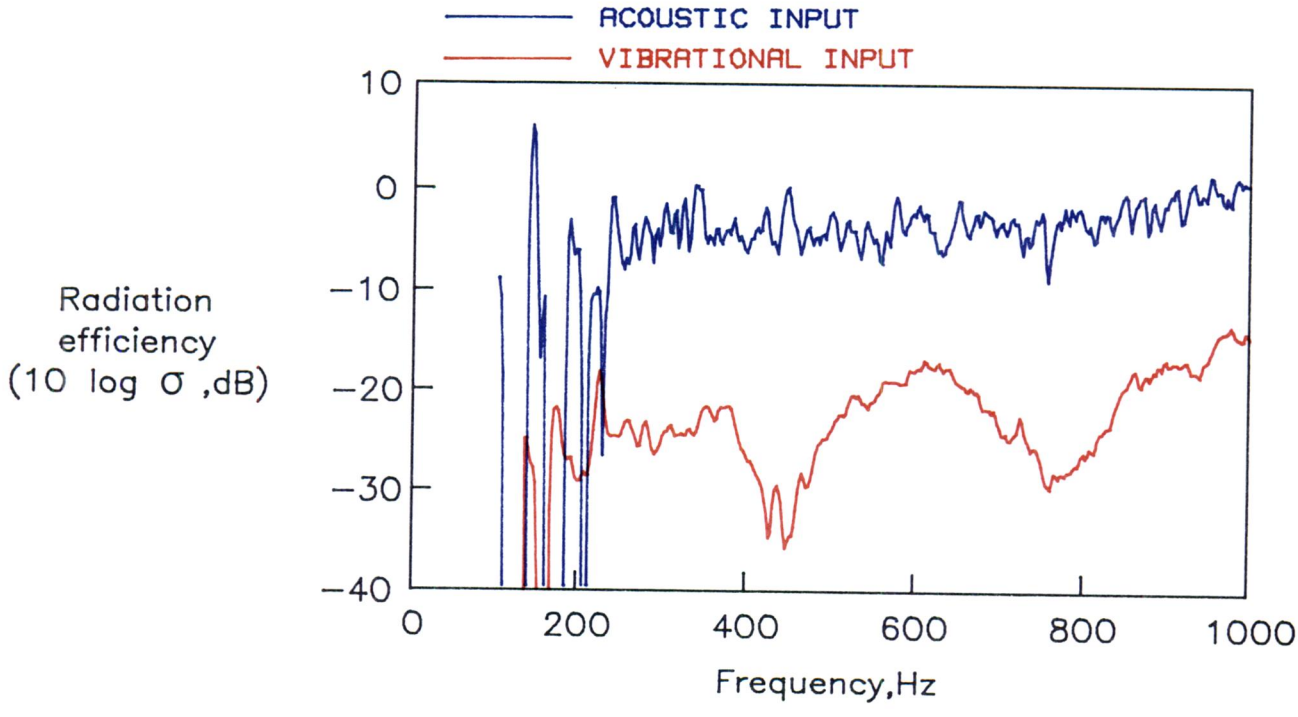

Figure 18.- Measured airborne and structureborne radiation efficiencies of the built-up aircraft panel with added damping. Panel 3.

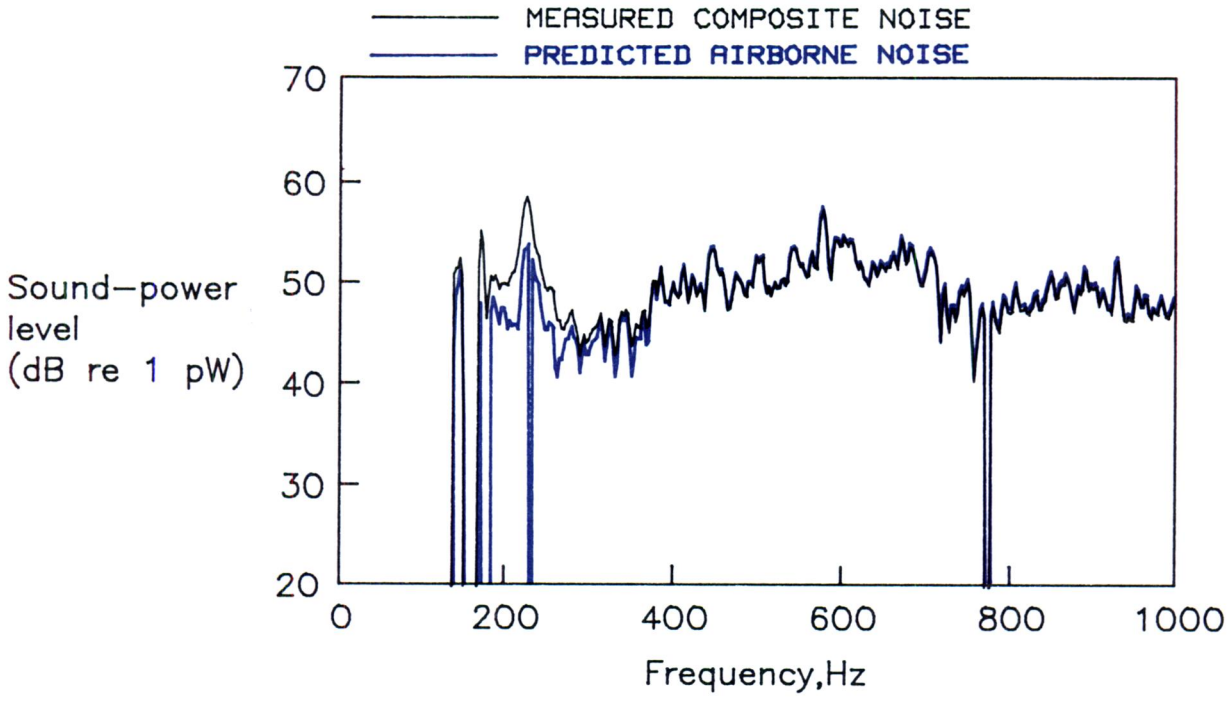

Figure 19.- Comparison of measured composite sound power and predicted airborne sound power for the built-up aircraft panel with added damping. Panel 3.

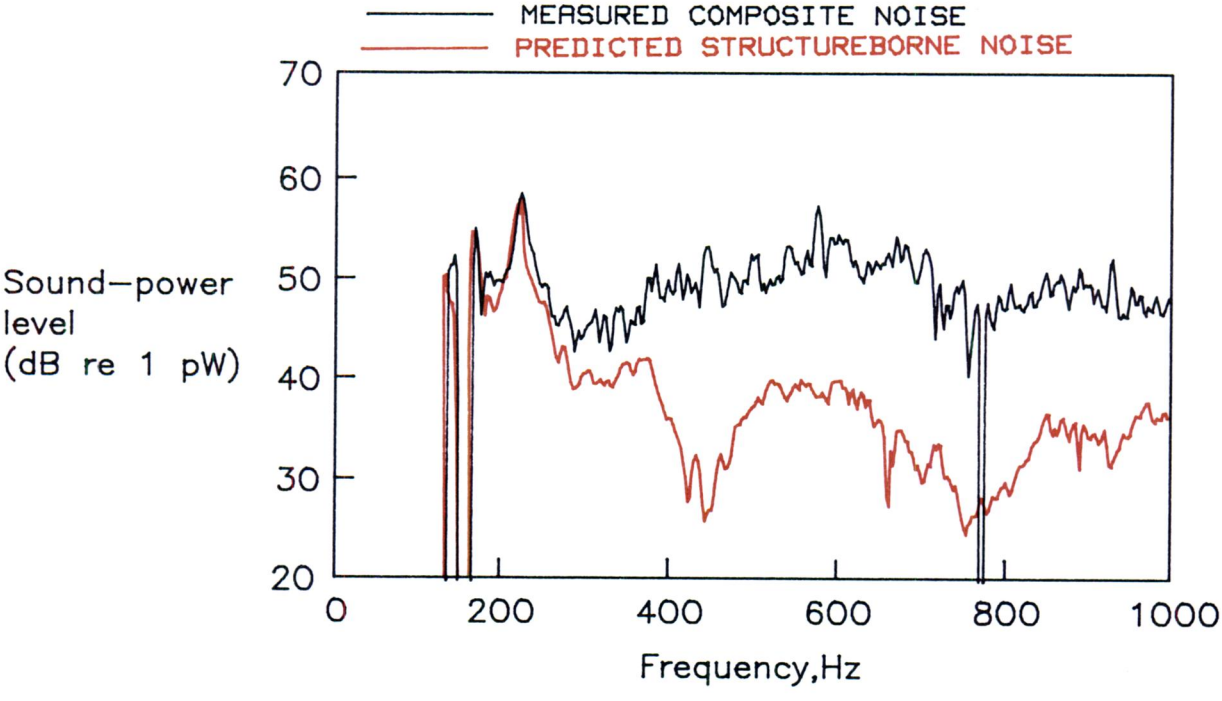

Figure 20.- Comparison of measured composite sound power and predicted structureborne sound power for the built-up aircraft panel with added damping. Panel 3.

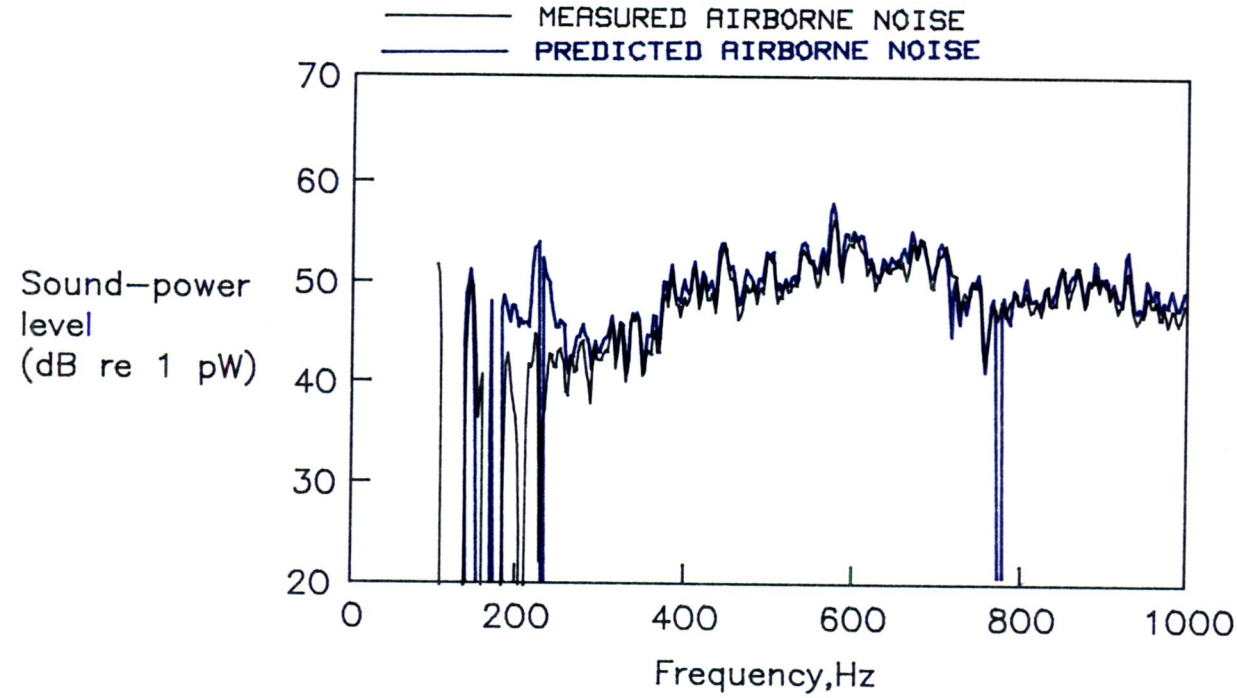

Figure 21.- Comparison of measured and predicted airborne sound powers for the built-up aircraft panel with added damping. Panel 3.

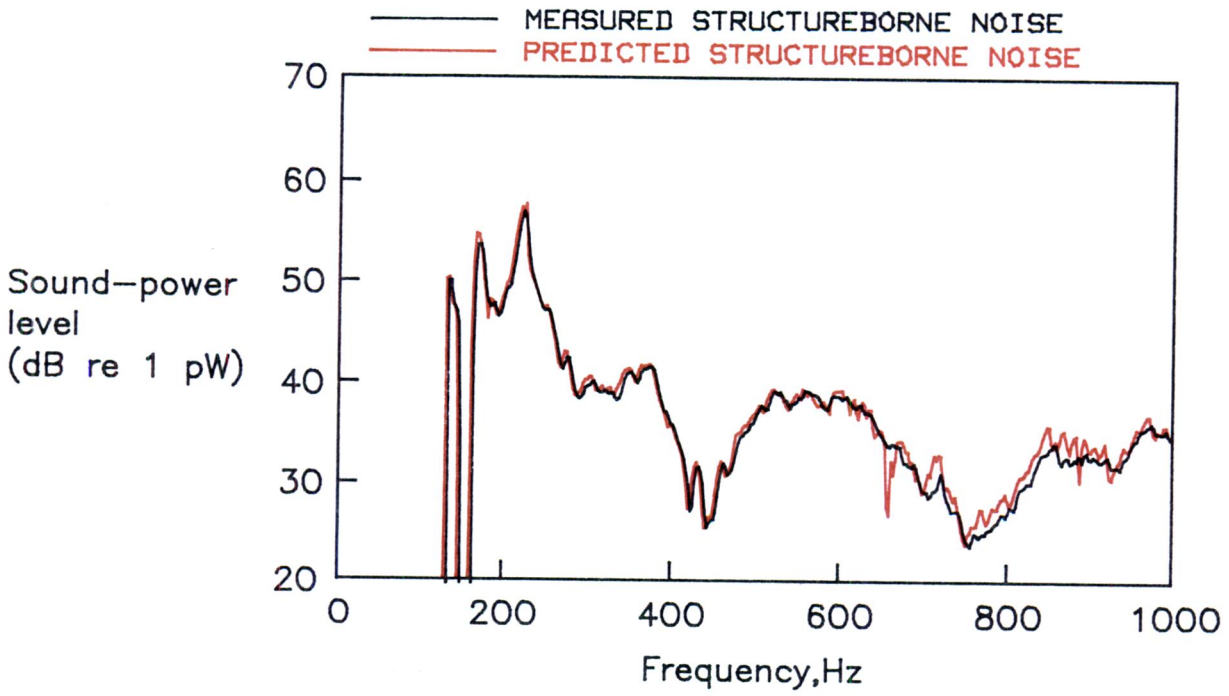

Figure 22.- Comparison of measured and predicted structureborne sound powers for the built-up aircraft panel with added damping. Panel 3.

1. Report No.	2. Government Accession No.	3. Recipient's Catalog No.
NASA TP-2079		

4. Title and Subtitle	5. Report Date
A NEW MEASUREMENT METHOD FOR SEPARATING AIRBORNE AND STRUCTUREBORNE NOISE RADIATED BY AIRCRAFT-TYPE PANELS	September 1982
	6. Performing Organization Code: 505-33-53-03
7. Author(s): Michael C. McGary	8. Performing Organization Report No.: L-15481
9. Performing Organization Name and Address: NASA Langley Research Center, Hampton, VA 23665	10. Work Unit No.
	11. Contract or Grant No.
12. Sponsoring Agency Name and Address: National Aeronautics and Space Administration, Washington, DC 20546	13. Type of Report and Period Covered: Technical Paper
	14. Sponsoring Agency Code

15. Supplementary Notes

16. Abstract

A new measurement method for separating airborne and structureborne noise radiated by aircraft-type panels has been developed. The accuracy of the method has been investigated for several different aircraft-type panels. The results of the study indicate that the method is quick, reliable, and inexpensive, and it can be applied to thin-shell structures of various designs.

17. Key Words (Suggested by Author(s))	18. Distribution Statement
Acoustic intensity Radiation efficiency Aircraft interior noise Propeller-driven aircraft Structureborne noise Propeller noise	Unclassified - Unlimited Subject Category 71

19. Security Classif. (of this report)	20. Security Classif. (of this page)	21. No. of Pages	22. Price
Unclassified	Unclassified	31	A03

For sale by the National Technical Information Service, Springfield, Virginia 22161

NASA-Langley, 1982